Journal of Advanced Research 25 (2020) 275–283

Contents lists available at ScienceDirect

Journal of Advanced Research

journal homepage: www.elsevier.com/locate/jare

Synthesis of elements with fractional-order impedance based on homogenous distributed resistive-capacitive structures and genetic algorithm

Pyotr Arkhipovich Ushakov [a], Kirill Olegovich Maksimov [a], Stanislav Valerevich Stoychev [a], Vladimir Gennadievich Gravshin [a], David Kubanek [b,*], Jaroslav Koton [b]

[a] Faculty of Instrumentation Engineering, Kalashnikov Izhevsk State Technical University, Studencheskaya 7, 426 069 Izhevsk, Russian Federation
[b] Faculty of Electrical Engineering and Communication, Brno University of Technology, Technicka 3082/12, 616 00 Brno, Czech Republic

GRAPHICAL ABSTRACT

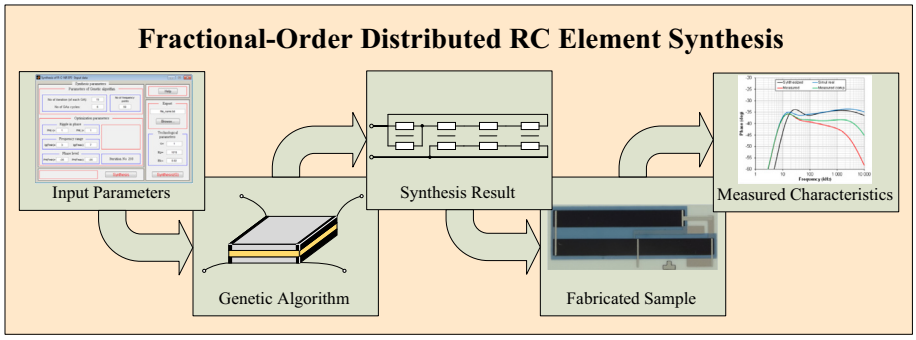

ARTICLE INFO

Article history:
Received 15 April 2020
Revised 10 June 2020
Accepted 22 June 2020
Available online 26 June 2020

Keywords:
Fractional-order impedance
Fractional-order element
Distributed resistive-capacitive structure
Circuit synthesis

ABSTRACT

The work proposes a synthesis method of capacitive fractional-order impedance element which is composed of homogenous distributed resistive-capacitive (RC) structures (lines). The method employs genetic algorithm and searches for optimal connection schemes and parameters of the partial RC structures. The synthesis algorithm is described in detail including the coding of the properties of the structures for the purpose of the genetic algorithm. The user interface of the design tool is introduced and the input and output parameters of the synthesis are explained. The algorithm was verified by computer simulations and particularly by measurements of element samples fabricated in thick-film technology. The results correspond to the required impedance characteristics, which confirm the validity of the synthesis method.

Introduction

Elements with fractional-order impedance (EFI) also known as fractional-order elements (FOEs) [1] or simply fractors [2] are very perspective building blocks for non-integer (i.e. fractional) order circuits and systems. These systems are described by fractional-order (FO) differential and integral equations, which is also the

Peer review under responsibility of Cairo University.
* Corresponding author.
E-mail address: kubanek@feec.vutbr.cz (D. Kubanek).

https://doi.org/10.1016/j.jare.2020.06.021
2090-1232/

case of many natural phenomena. The characteristics and properties of FO systems are not realizable by their integer-order counterparts or at the cost of increased complexity or worse accuracy. Various disciplines take advantage of utilizing FO systems as they provide an accurate mathematical and electrical equivalent model of a real-world system or improved ability to control it [3–5].

Based on the similarity with the standard capacitor and inductor, the mathematical models of EFI, namely FO capacitor and FO inductor, can be represented using the concept of fractional differentiation [6] as follows

$$i_{C_\alpha} = C_\alpha \frac{d^\alpha u_{C_\alpha}}{dt^\alpha}, \tag{1}$$

$$u_{L_\beta} = L_\beta \frac{d^\beta i_{L_\beta}}{dt^\beta}. \tag{2}$$

Transforming (1) and (2) to the s-domain, the relations for impedance of the FO elements have the form

$$Z_{C_\alpha}(s) = \frac{1}{s^\alpha C_\alpha}, \tag{3}$$

$$Z_{L_\beta}(s) = s^\beta L_\beta, \tag{4}$$

where s is the Laplace operator (complex frequency), the constants C_α and L_β are also referred to as pseudo-capacitance and pseudo-inductance having units $F{\cdot}s^{\alpha-1}$ and $H{\cdot}s^{\beta-1}$, respectively. The real positive exponents α and β are the fractional orders in the range (0; 1). When substituting $s = j\omega$ into (3) and (4) we obtain an important feature of these elements: the phase of the impedance of FO capacitor is constant and equal to $-\alpha\pi/2$, whereas the phase of the impedance of FO inductor equals to $\beta\pi/2$ independent of frequency. Hence, such elements are also called constant phase elements (CPEs). More attention is given to FO capacitors than FO inductors, as it is also in integer-order domain. The bulky and difficult to integrate inductors caused higher interest in the design of integer-order systems with capacitors and therefore also the FO systems more often employ FO capacitors. Hence, when we refer to the term EFI from here on, we mean capacitive EFI, i.e. FO capacitor.

The recent survey on possible techniques and approaches to design single or multi-component FO capacitors as being proposed by different research groups can be found in [1]. Here the authors state that particularly single-component EFIs are being researched upon vigorously. They are mostly based on electrochemical principles utilizing various chemical substances, for example porous polymer materials [7], nanocomposites of conductive particles in dielectric [2,8,9] or layered structures in dielectric [10,11]. These elements are mostly designed on the basis of choice of suitable materials, their arrangement and fabrication technologies by conducting many experiments, but no algorithms using exact circuit-theory laws are employed. The experimental results are used to derive approximated design equations by regression methods. Common features of these elements are low range of the fractional order α and/or narrow frequency band of the constant phase shift. None of the elements is currently commercially available in the solid-state form and most of them also do not have any dependence relation between the order α and the electrochemical parameters [1].

Thus a common way to obtain EFIs is their emulation by multi-component integer-order passive or active circuits. The method is based on the approximation of the term s^α (or s^β) in the impedance function by integer-order rational function [12–16]. This function is then implemented for example in the form of Foster or Cauer passive ladder networks with resistors and standard capacitors (or inductors) with lumped parameters [17]. However, the values of these resistors and capacitors must be precise to obtain the required accuracy of approximation [17]. Furthermore, when the values of α are required being close to 0 or 1, the ratio of the resistances and capacitances is very high [18]. This makes the integration in the film or semiconductor technology very difficult or even impossible. Also, the passive emulation structures cannot be tuned electronically. The last two drawbacks mentioned are eliminated by active emulation circuits, which are usually based on state-variable structures whose transfer function equals to the required integer-order rational impedance function [19]. These circuits can offer electronic adjustability thanks to the controlled active elements employed and are suitable for integrated implementation. The obvious common feature of these emulation techniques is their validity only in a limited frequency band.

Impedance synthesis with distributed RC structures

The idea of realizing impedances with given characteristics by resistive-capacitive (RC) circuits with distributed parameters was put forward already in the last century, see e.g. [20–22]. The synthesis method is based on utilizing homogenous RC lines of the form R-C-0 (resistor-capacitor-conductor) described by voltage-current relations containing hyperbolic trigonometric functions. The s-domain input impedance of a circuit of any complexity containing these R-C-0 lines multiplied by $\sqrt{s}$ can be written as a rational function in t-domain, whereas the relation $t = \tanh\sqrt{sRC}$ holds for the transition between the domains. As a result, the R-C-0 lines with shorted output in s-domain are transformed to standard inductors (L) in t-domain and R-C-0 lines with open output are transformed to standard capacitors (C). Therefore, the desired synthesized impedance in s-domain multiplied by $\sqrt{s}$ is approximated by a rational function in t-domain, which is after a suitable expansion (sum of fractions or continued fraction) implemented by LC circuit. The final synthesis step is the inverse conversion within which the inductors and capacitors are replaced by shorted and opened R-C-0 lines respectively [20–22].

However, the synthesis of EFI is not taken into account in the aforementioned works, as well as the problem of its physical realization by film or semiconductor RC lines is not addressed. Therefore, we have investigated the possibility of EFI synthesis based on R-C-0 lines and evaluated the physical realization using modern film technologies. It turned out that the implementation is impossible under the existing restrictions on the specific parameters of resistive and dielectric materials, since it leads to element sizes that are comparable with the dimensions of neither ordinary discrete elements, nor integrated circuits.

Next to the basic R-C-0 lines, also other types of RC lines were analyzed. As it will be discussed in the section below, the R-C-NR layer structure shows to be suitable for efficient design of EFIs [23–25]. It contains two resistive layers with resistances R and $N \times R$, a capacitive (dielectric) layer with capacitance C between them and four connection terminals as shown in Fig. 1.

Analyzing the structure in Fig. 1(b), the relation between the currents I_1, I_2, I_3, I_4 and voltages V_1, V_2, V_3, V_4 can be described using admittance matrix as [28]

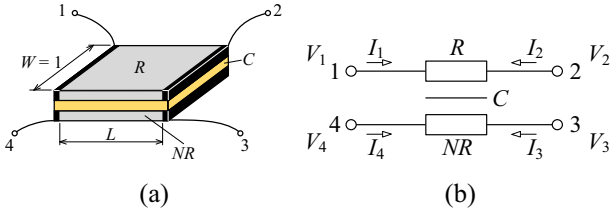

Fig. 1. (a) The 3D view of R-C-NR structure, (b) its equivalent schematic.

$$\begin{bmatrix} I_1 \\ I_2 \\ I_3 \\ I_4 \end{bmatrix} = \frac{1}{(1+N)R} \begin{bmatrix} \frac{\theta}{\tanh\theta}+N & -\frac{\theta}{\sinh\theta}-N & \frac{\theta}{\sinh\theta}-1 & 1-\frac{\theta}{\tanh\theta} \\ -\frac{\theta}{\sinh\theta}-N & \frac{\theta}{\tanh\theta}+N & 1-\frac{\theta}{\tanh\theta} & \frac{\theta}{\sinh\theta}-1 \\ \frac{\theta}{\sinh\theta}-1 & 1-\frac{\theta}{\tanh\theta} & \frac{\theta}{\tanh\theta}+\frac{1}{N} & -\frac{\theta}{\sinh\theta}-\frac{1}{N} \\ 1-\frac{\theta}{\tanh\theta} & \frac{\theta}{\sinh\theta}-1 & -\frac{\theta}{\sinh\theta}-\frac{1}{N} & \frac{\theta}{\tanh\theta}+\frac{1}{N} \end{bmatrix} \begin{bmatrix} V_1 \\ V_2 \\ V_3 \\ V_4 \end{bmatrix}, \quad (5)$$

where

$$\theta = \sqrt{j\omega RC(1+N)}. \quad (6)$$

As the R-C-NR structure has fourth-order admittance matrix, the number of different synthesizable impedances is significantly larger than for RC lines of the form R-C-0. However, the application of impedance synthesis techniques based on the domain transformation requires knowledge, which circuits with R, C, and L elements in the transformed domain correspond to different R-C-NR-based circuits in the *s*-domain. In addition, it is necessary to modify these synthesis methods to provide connections of R-C-NR structures with FO impedance.

Therefore, we have developed a structural-parametric synthesis method of EFI composed of specifically connected four-terminal homogeneous R-C-NR structures (lines) which has been already briefly introduced in [23]. This method profits from genetic algorithm, is implemented as a computer program and has shown its effectiveness based on our experience. The aim of this work is to describe this synthesis method in more detail with emphasis on coding the parameters of distributed RC structures for the purpose of the algorithm and on the detailed description of the algorithm itself. The synthesis method is also evaluated and verified in the subsequent sections.

Fractional-order impedance synthesis based on R-C-NR structures

General assumptions of synthesis

The classic problem of an electric circuit synthesis is formulated as follows: it is necessary to find a circuit and the parameters of its elements that provide the desired output response to a certain input signal. The synthesis of any technical object involves creating its structure and determining its parameters. These two parts of the synthesis are called *structural* and *parametric* synthesis. The *structure of the object* determines how it is constructed, what physical parts it consists of and how these parts are related. The *parameters of the object* are understood as structural and electrophysical parameters of its parts.

We will consider the synthesis of EFI based on R-C-NR structures with distributed parameters. Obviously, the *structure* of the element will be given by the interconnection of the particular R-C-NR structures resulting in the connection diagram of the components of the EFI. The *parameters* will include the properties of the resistive and dielectric layers, i.e. their lengths *L* (relative to the unity width *W* = 1 of all R-C-NR structures) and electrophysical characteristics. Considering that EFI is supposed to be manufactured in one of the known integrated technologies, it is advisable that the electrophysical characteristics of the layers are the same for all the parts of the element.

The synthesis objective is the constant phase level (with defined error) of the input impedance of the element in the range from 0 to –90°. As constraints we set the frequency range of phase constancy, restrictions on the ratio of the resistivity of the top and bottom resistive layers *N*, the boundaries of resistance and capacitance per unit length, and fixed values of other parameters in the equivalent circuit model of the RC line that we have previously published in [23].

The reason for choosing the phase angle as the synthesis criterion is that it provides higher accuracy in the circuit synthesis compared to magnitude. Also the fractional order α is more sensitive to a change of the phase angle than to the magnitude slope of the frequency response. Determining and setting the impedance magnitude is possible after the synthesis by the resistance and capacitance of the layers as described in more detail in section "Verification of the Synthesis Program".

The described technique is not directly applicable to the design of fractional-order inductors, as only resistive and capacitive layers are considered. However, availability of fractional-order capacitor allows obtaining fractional-order inductor by impedance transformation using an active circuit, such as generalized impedance converter (GIC) or gyrator, see e.g. [26].

Design steps of R-C-NR EFI synthesis program

The properties of EFI based on R-C-NR structures are described by a large number of internal factors. For example there are more than 10 thousand variants of connection schemes for four four-terminal R-C-NRs, not including combinations of structural and electrophysical parameters of the layers. Therefore, for such objects it is not rational to use the common methods of minimizing objective functions. In such cases the most effective are the heuristic optimization methods, in particular evolutionary algorithms based on the generate-and-test principle. One of these methods is the genetic algorithm (GA) [27], which we also use here for the synthesis of EFI. The synthesis method is designed according to the following steps:

1. Specification of coding of R-C-NR EFI factors.
2. Development of the general structure of GA, reflecting the sequence of genetic operations.
3. Development of a synthesis program for R-C-NR EFI.
4. Study of potential possibilities and determination of optimal parameters of GA, providing the maximum probability of synthesis of physically realizable R-C-NR EFI with given characteristics.

Coding of R-C-NR EFI factors

All factors that fully and unambiguously describe the design of the R-C-NR EFI can be represented by a set $\mathbf{\Psi}$ of the form

$$\Psi = \mathbf{P} \cup \mathbf{C}, \quad (7)$$

where **P** is a set of parametric factors, i.e. the parameters of individual R-C-NR structures. The set **C** includes circuit structure factors covering the interconnections of adjacent R-C-NRs and their connection to the overall input nodes of the synthesized EFI denoted here as *in* and *gnd*. The set **P** can be further defined as

$$\mathbf{P} = \mathbf{N} \cup \mathbf{L}, \quad (8)$$

where the sets **N** and **L** include the values of the parameters *N* (ratio of the resistivity of the top and bottom layers) and *L* (relative length of the layers) of each R-C-NR. The set **C** can be specified as

$$\mathbf{C} = \mathbf{E} \cup \mathbf{A} \cup \mathbf{B}, \quad (9)$$

where the set **E** includes valid interconnection schemes of adjacent R-C-NRs, the set **A** determines the nodes of adjacent R-C-NRs connected to the *gnd* node, and the set **B** defines connections of external terminals of the series of R-C-NR structures.

Since the program for EFI synthesis has been developed in the MATLAB® environment, it is advisable to express the introduced sets of the EFI factors in matrix format.

Coding of parametric factors

The coding of parametric factors consists in determining the form for representing the parameters of the set **P** given by (8) and the range of allowed values for the elements of each of the subsets. The parameters N and L of the particular connected R-C-NR structures are expressed in the matrix form:

$$\mathbf{N} = [N_1 \quad N_2 \quad \dots \quad N_n], \quad \{N_1, N_2, \dots, N_n\} \in \mathbb{R}_N^+, \tag{10}$$

$$\mathbf{L} = [L_1 \quad L_2 \quad \dots \quad L_n], \quad \{L_1, L_2, \dots, L_n\} \in \mathbb{R}_L^+. \tag{11}$$

Here n is the total number of the R-C-NR structures, which was set to 4 in our EFI synthesis tool. The symbols $\mathbb{R}^+$ with the corresponding subscripts represent positive real numbers and the allowed ranges of N and L according to the structural and technological limitations determined by the manufacturing technology. The matrix form of the chromosome expressing the parametric factors can be written as

$$\mathbf{PCh}_i = \begin{bmatrix} N_1 & N_2 & N_3 & N_4 \\ L_1 & L_2 & L_3 & L_4 \end{bmatrix}, \tag{12}$$

where the index i indicates one set of the parameters that is used in the current iteration of GA.

In addition to the above defined N and L parameters, there are other important parameters in the mathematical model of the R-C-NR structure as described in [23]. It is in particular the resistance of the top resistive layer (R_0) and the capacitance between the resistive layers (C_0) per unity length L. As the parameters R_0 and C_0 only shift the synthesized impedance characteristic along the frequency axis and set the impedance magnitude without affecting the shape of the characteristic, they were excluded from the set **P** for sake of simplicity. Other parameters are the transition resistance between the resistive and capacitive layers, the leakage resistance of the capacitive layer and resistance of metal contacts (see section "Development of Genetic Algorithm for the Synthesis of EFI"). These parameters depend on the manufacturing technology and therefore their values are automatically set in the algorithm as the most representative for the selected technology.

Coding of circuit factors

To code the circuit structure factors it was necessary to determine the form for representing the parameters of the set **C** (9) and the range of permissible values for the elements of each of the subsets. The valid interconnection schemes of two adjacent R-C-NR structures k and $k + 1$ are shown in Fig. 2(a) and the corresponding coincidence matrices defining each variant of the interconnections are stated in Fig. 2(b).

The elements of the set **E** coding these interconnections are formed by matrices $\mathbf{E}_k$ containing only two values α_1 and α_2 equal to the row and column of the position of the coincidence matrix in Fig. 2(b):

$$\mathbf{E}_k = [\alpha_1 \quad \alpha_2]; \alpha_1 = \{1,2\}; \ \alpha_2 = \{1,2,3,4\}; \ k = 1,2,\dots,n-1. \tag{13}$$

Thus each element of the set **E** corresponds to the coincidence matrix that uniquely specifies the switching of the terminals of adjacent R-C-NR structures. Based on the union of the coincidence matrices, a global coincidence matrix is created that describes connection of all n (in our case 4, as mentioned above) R-C-NR structures. Finally, a global admittance matrix of the whole element is created.

Some nodes in the circuit interconnected according to the set **E** can be grounded (i.e. connected to the *gnd* input node), which provides additional degree of freedom. This is defined in the set **A** whose elements are represented by matrices $\mathbf{A}_k$ of dimension 4×1. The elements in the matrix $\mathbf{A}_k$ have unity values in the rows corresponding to the numbers of grounded nodes as apparent in the examples in Fig. 3. The index k here also ranges from 1 to $n - 1$.

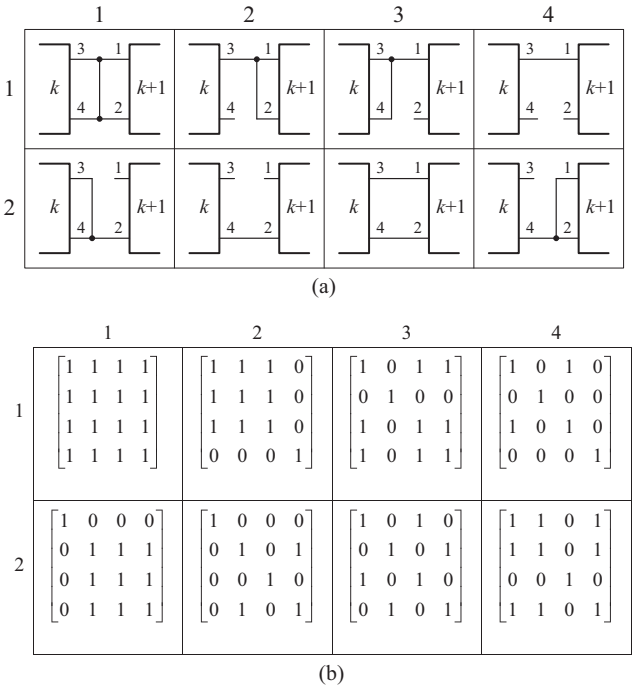

Fig. 2. (a) Valid interconnections of adjacent four-terminal R-C-NR structures and (b) their respective coincidence matrices.

Thus information about the connection of adjacent R-C-NR structures is presented by a pair of matrices $\mathbf{E}_k$ and $\mathbf{A}_k$ which forms a gene. The array of (n-1) pairs (in our case of 3 pairs) of matrices $\mathbf{E}_k$ and $\mathbf{A}_k$ forms a chromosome reflecting the internal connections

$$\mathbf{CCh}_i = \{(\boldsymbol{E}_1, \boldsymbol{A}_1), (\boldsymbol{E}_2, \boldsymbol{A}_2), (\boldsymbol{E}_3, \boldsymbol{A}_3)\}. \tag{14}$$

The set **B** defines connection of external nodes of the series of R-C-NR structures. Any of the external nodes can be connected to: EFI input node (*in*); ground node, i.e. the second EFI input node (*gnd*); another external node (*con*); no node, i.e. left floating (*float*). The set **B** is then represented as the matrix

$$\mathbf{B}_i = \begin{bmatrix} in_1 & in_2 & in_3 & in_4 \\ gnd_1 & gnd_2 & gnd_3 & gnd_4 \\ float_1 & float_2 & float_3 & float_4 \\ con_1 & con_2 & con_3 & con_4 \end{bmatrix}, \tag{15}$$

where the number of rows equals to the number of possible states of the external nodes (i.e. *in*, *gnd*, *float*, *con*) and the number of columns corresponds to the number of external nodes of EFI (which is always 4). Assigning an external node to one of the four states is performed by setting the unity value of the matrix element in the intersection of the row with the selected state and of the column corresponding to the node number. Since only one state can be assigned to any node, each column of the matrix $\mathbf{B}_i$ contains only one element with the value one. The remaining elements are zero. An example of matrix coding is shown in Fig. 4.

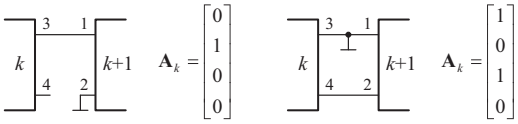

Fig. 3. Examples of R-C-NR terminals grounding and the respective matrices $\mathbf{A}_k$.

To obtain only valid external EFI switching schemes the following rules for the formation of elements of the set **B** were defined:

- there must be at least one *in* node,
- there must be at least one *gnd* node,
- the number of nodes with *con* status cannot be less than two.

Thus, when coding circuit properties by the chromosome structures, genes appear that carry information that is not represented in the form of decimal numbers or bit sequences, as is usual in genetic algorithms. The information has the form of hierarchical structures that include elements of sets in the form of matrices related to electrical circuits.

Development of genetic algorithm for the synthesis of EFI

The mathematical description of GA for EFI synthesis has the general form

$$\mathrm{GA} = \{P^0, r, l, sl, Fit, cr, m, rj\}, \tag{16}$$

where P^0 is the initial population, r is the population size, l is string length coding the solution, sl is selection operator, Fit is the fitness function, cr is crossover operator, m is the mutation operator, and rj is the rejection operator. Note that classic genetic operators are used. The peculiarity is that the algorithm is used for synthesis of a distributed circuit element consisting of segments of RC lines, which are interconnected in a specific way and have specific electrical parameters. Since the model of such a line is described by a conductivity matrix, the coding of the element properties (internal connection and electrical parameters) and genetic operators are performed in matrix form. To the best of the authors' knowledge, this kind of implementation of genetic operators has not been previously used.

The fitness function *Fit*, calculated for each individual in the population, determines the probability of keeping this individual in the population or its removal as an erroneous decision that does not improve the population. The requirements for the frequency response of the impedance phase of the synthesized EFI are determined in the form of a window as seen in Fig. 5.

The width of the window determines the frequency range of phase constancy ($\omega_{\min}RC$ to $\omega_{\max}RC$), and its height defines the permissible deviation ($\pm\varepsilon$) from a given level of the constant phase φ_c. Regardless of the shape of the phase response, it is important that all its points fall into this window. Therefore, the easiest way to evaluate the fitness function is to determine the number of the phase response points, which are located within a given window. In this case the fitness function can be specified by the formula

$$Fit = \sum_{i=1}^{N_\omega} \beta_i, \tag{17}$$

where

$$\beta_i = \begin{cases} 1, & \text{if } |\varphi_c - \varphi_i| < \varepsilon \\ 0, & \text{if } |\varphi_c - \varphi_i| \geqslant \varepsilon \end{cases} \text{ for } \omega_{\min}RC \leqslant \omega_i RC \leqslant \omega_{\max}RC,$$

φ_i is the value of the impedance phase of the evaluated EFI variant at a frequency $\omega_i RC$, i is the number of the frequency point in the given frequency range from $\omega_{\min}RC$ to $\omega_{\max}RC$; i = 1, 2, …, N_ω, whereas N_ω is total number of frequency points. In the example in Fig. 5 based on the relation (17) we get Fit = 11 (with a maximum possible value of 17). The value of φ_i is computed by the methods of circuit theory utilizing the admittance matrix of one R-C-NR structure appearing in (5) and parametric and circuit factors given by the sets **P** and **C**.

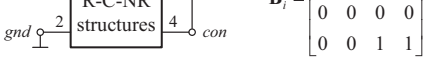

$$\mathbf{B}_i = \begin{bmatrix} 1 & 0 & 0 & 0 \\ 0 & 1 & 0 & 0 \\ 0 & 0 & 0 & 0 \\ 0 & 0 & 1 & 1 \end{bmatrix}$$

Fig. 4. Example of coding the $\mathbf{B}_i$ matrix.

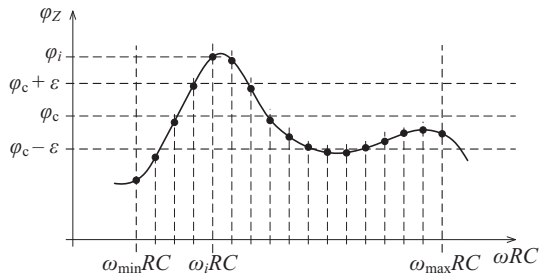

Fig. 5. Example of the allowed window of the phase response for fitness function calculation.

When developing the general structure of GA, it was taken into account that the elements of the sets **P** and **C** have different physical nature, different mathematical representations of genes and chromosomes, as well as different algorithms for implementing crossover and mutation operators. Thus the GA was implemented as multi-stage as seen in the flow-chart of the proposed algorithm in Fig. 6.

At the beginning of the synthesis, the allowed impedance phase window and the genetic algorithm parameters x, y (maximum number of iterations) and δ (threshold for *Fit* function) are defined by the user. The program continues with generating random elements of the set **P**. The block "Formation of parental individuals with parameters from the set **C**" deals with creating the initial parental pair by random generation of elements of the set **C** and computing their fitness functions in cycles until two individuals (i.e. parents) are found with the *Fit* value higher than a threshold δ_1, which is specified by the program developer (see section "Evaluation of the Algorithm"). A similar block "Formation of parental individuals with parameters from the set **P**" is also present in the program which randomly generates elements of the set **P** until their *Fit* value reaches a threshold δ_2. The choice of parental individuals ensures initial approach of the fitness function to the optimum and essentially influences the fitness function growth in the following parts of the algorithm.

From this point the program is divided into two genetic algorithms GA(**C**) and GA(**P**). The first one searches for the optimized internal and external connections and the second one deals with optimizing the parametric factors of the R-C-NR EFI. The parental arrays $\mathbf{CCh}_\mathrm{A}$ and $\mathbf{CCh}_\mathrm{B}$, see relation (14), and the set **B**, see (15), are processed by GA(**C**) whereas the parametric factors are unaffected. In the case of GA(**P**), the parental arrays $\mathbf{PCh}_\mathrm{A}$ and $\mathbf{PCh}_\mathrm{B}$, see (12), are optimized without altering the connections. The first block of both GAs is "Crossover", which performs a one-point crossover operation with a random choice of crossing-over point. Offsprings are formed as a result of mutual exchange of genes located to the right of the crossing-over point. The following block "Mutation" consists in replacing one or more genes of the parental individual with genes randomly selected from a permitted range. This ensures maintaining a sufficient diversity of the genetic material of the population. A total of 15 offspring individuals are created during the crossover and mutation. In the case of GA(**C**) the arrays $\mathbf{CCh}_\mathrm{A}$ and $\mathbf{CCh}_\mathrm{B}$ are subject to crossover and mutation and after that the set **B** is randomly generated for each of the 15 individuals.

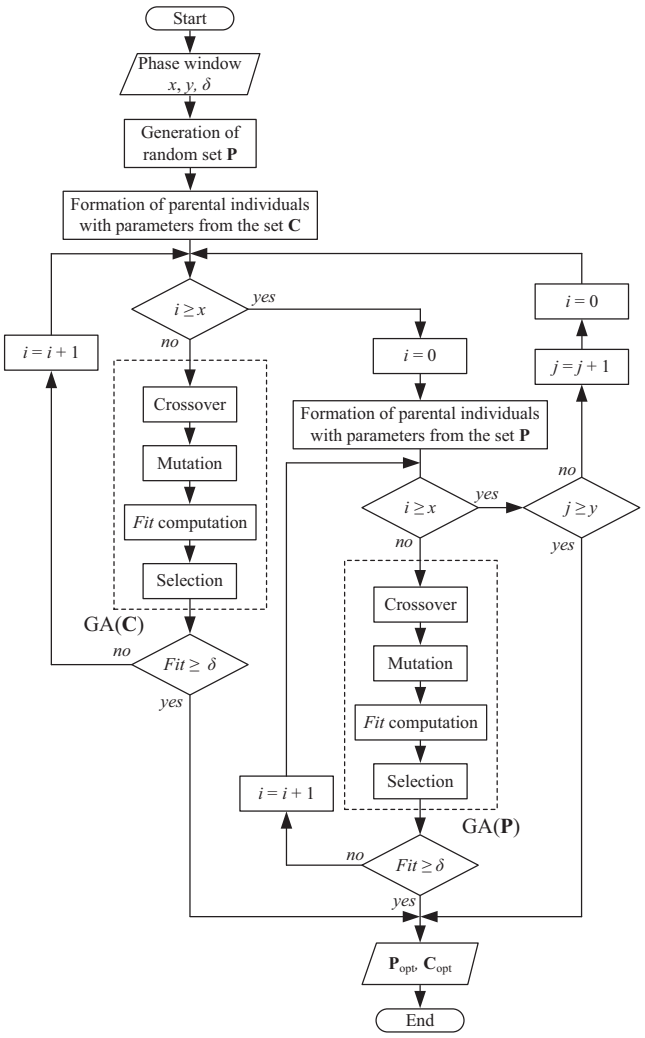

Fig. 6. Flow-chart of algorithm for R-C-NR EFI synthesis.

The GA continues with "Selection" block, where from the offsprings two different individuals are selected that form the input parental pair of the next cycle of GA. The selection is fitness proportionate, i.e. the Fit_q value of an individual q is used to determine the probability p_q of selection of this individual:

$$p_q = \frac{Fit_q}{\sum_{i=1}^{r} Fit_i}, q = 1, 2, \ldots, r, \tag{18}$$

where r is the size of population equal to 15 in this work.

It is also possible to utilize "Rejection" operator in the algorithm, which eliminates a given number of unsuccessful solutions with the worst values of fitness function. However the rejection is not activated in the described program version, because the "Selection" operator selects only 2 individuals which proceed directly as parents to the next GA cycle, so there is no need to reject any solutions.

The algorithm GA(**C**) and also the whole synthesis program are terminated when the *Fit* value of the two selected individuals reaches a certain threshold δ. For the best results, δ is equal to the total number of frequency points N_ω, hence the user sets N_ω in the user interface. Another condition of termination of GA(**C**) is reaching a given number of iterations x. In this case the synthesis continues with execution of the algorithm GA(**P**) with fixed elements of the set **C**. As a result, the optimized parameters of the set **P** are found. The termination conditions of GA(**P**) are the same as in the case of GA(**C**). If the algorithm GA(**P**) is terminated by exceeding the allowed number of iterations x (and *Fit* value does not reach δ) the program proceeds again with GA(**C**). Both GAs can be alternated in this way up to y times, provided that the *Fit* value still does not reach δ.

Based on the proposed algorithms, the main program modules and user interface for working with the synthesis program in interactive mode have been developed. The user interface dialog boxes are shown in Fig. 7.

The dialog box in Fig. 7(a) is used to set the requirements for the phase response (in degrees) of the input impedance of the EFI in the form of a window. The window height, i.e. the allowed ripple of the phase response, is set by positive "PH(+)" and negative "PH(−)" deviation from the mean phase value at the respective frequency. The mean phase values at the lower and upper frequency boundaries are given by "PH(Fmin)" and "PH(Fmax)", respectively. These values are equal for fractional orders that are real numbers. The values "lg(Fmin)" and "lg(Fmax)" are logarithms of lower and upper boundary frequencies (in Hz), which define the frequency range of phase constancy. By setting these values, it is possible to change the frequency bandwidth of the window of the phase constancy and also to shift it along the frequency axis. The values "No of iteration (of each GA)" and "No of GAs cycles" correspond to x

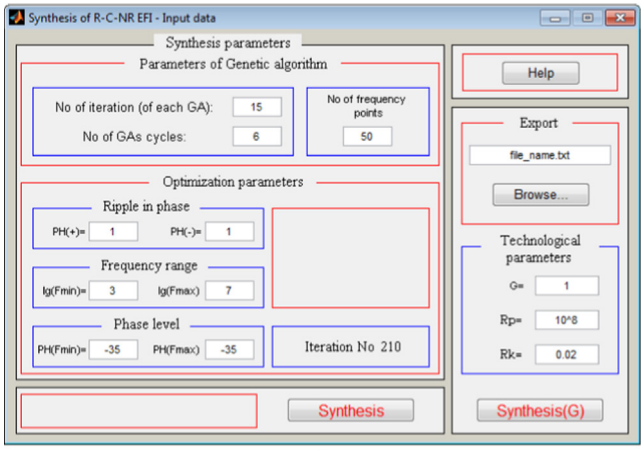

(a)

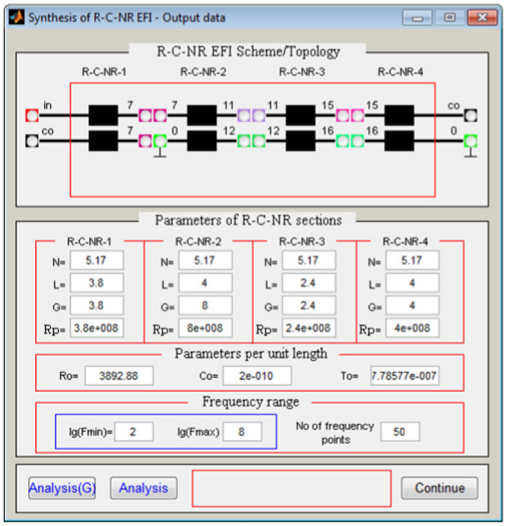

(b)

Fig. 7. Dialog windows of the EFI synthesis program; (a) input and (b) output data of synthesis.

and y respectively in Fig. 6. The "No of frequency points" specifies N_ω.

The program provides two synthesis modes. The button "Synthesis" executes the synthesis without taking into account the technological parameters, whereas "Synthesis(G)" considers these parameters. The technological parameter "G" is the coefficient of proportionality between the transition resistance between the resistive and capacitive layers and the resistance of the top-layer, "R_p" is the leakage resistance of the capacitive layer, and "R_k" is the resistance of metal contacts. These parameters are defined for elemental part of the multilayer R-C-NR network as presented in [23]. They depend on the manufacturing technology and therefore their values are to be determined, for example by experimental measurement of test samples. The values stated here (G = 1, $R_p = 10^8$, $R_k = 0.02$) are typical for thick-film technology. The synthesis with these technological parameters utilizes definition of θ different from (6), namely

$$\theta = \sqrt{\frac{R(1+N)(1+j\omega CR_p)}{R_p + RG(1+N)(1+j\omega CR_p)}}. \quad (19)$$

The program provides the following restrictions related to the structural and technological feasibility of the synthesized R-C-NR EFI: the values of the N parameters for all sections are the same (since all layers of the sections are expected to be performed in one technological cycle) and the range of possible values of the parameter L is from 0.1 to 10.

When one of the conditions for exiting the synthesis program is fulfilled, the dialog box with synthesis results is displayed (Fig. 6 (b)) along with the impedance phase graph of the synthesized EFI. The displayed frequency range and the parameters of the R-C-NR structures can be changed in this box by user. The synthesis can continue with the changed parameters (but without changing the connections of particular R-C-NR structures) when Continue is pressed. In addition, this box also provides the possibility of quick analysis of the EFI model with synthesized or user-modified parameters both taking into account the technological parameters "Analysis(G)", and without taking them into account "Analysis".

Evaluation and verification

Evaluation of the algorithm

The genetic algorithm is a pseudo-random optimization method. The level of convergence of the resulting function to the objective function (which is measured by the *Fit* value) depends on a number of parameters characterizing the GA, particularly on the choice of the number of individuals in the population (r), number of GA iterations (x, y), and the minimum threshold values of the fitness function δ_1 and δ_2 utilized during the formation of initial parental individuals. The effects of setting the δ_1 and δ_2 threshold values ($\delta_1 = \delta_2$) on the average GA execution time and final obtained *Fit* value are shown in Fig. 8. The testing was performed with DELL Vostro 1220 laptop (Intel® Core™2 Duo Processor T6670, 4 GB DDR2) and MATLAB 7.1.

The results presented in Fig. 8 showing the average performance of the algorithm are valid for the following synthesis parameters: the level of the constant impedance phase in the range from −5° to −85° in increments of 5°, allowed phase deviation ±1°, frequency bandwidth of the constant phase 2 decades, the number of points on the frequency axis 50, the number of GA iterations 200. The averaging of the results was carried out with 100 runs of the program for each level of the constant phase and each value $\delta_1 = \delta_2$. The *Fit* value (i.e. the convergence of GA) increases with increasing the values δ_1 and δ_2, however, the synthesis time also increases. Note that when δ_1 and δ_2 values are higher than 12,

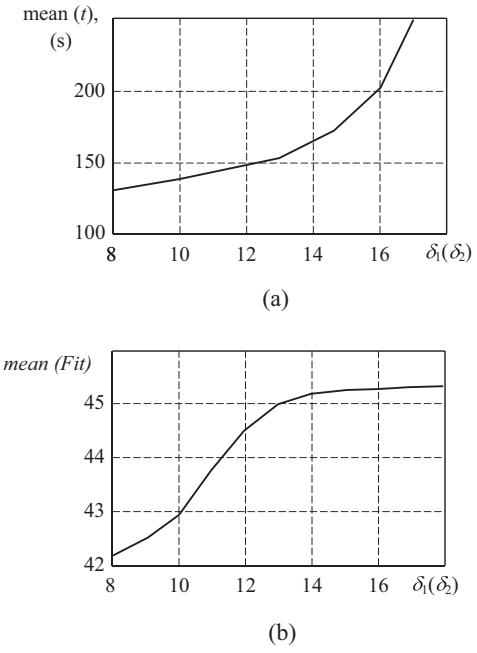

Fig. 8. Analysis of the influence of the selected δ_1 and δ_2 values on the GA properties (a) average time of execution; (b) average *Fit* value.

the convergence improves only slightly and the execution time grows rapidly. Therefore a further increase of δ_1 and δ_2 is not advisable. Based on our observations described above, for the purpose of our current tool to design EFIs, the values of δ_1 and δ_2 were set to 6 and 8 respectively.

With an increase in the number of iterations, the GA convergence increases, however, the synthesis time also increases. While evaluating the performance of the synthesis program, we also observed that for the total number of iterations, i.e. $2x(y + 1)$, above 200, the convergence rate of the GA increases only slightly, therefore, a further increase in the number of iterations is not advisable.

Verification of the synthesis program

The synthesis of EFI was carried out for the required constant phase −35° with deviation ±1° in the frequency range 10^3–10^7 Hz and 50 frequency points. The resulting element is described by the topology in Fig. 9 and the parameters N = 5.17, L_1 = 3.8, L_2 = 4, L_3 = 2.4, L_4 = 4. The original generated values of the layer resistance R_0 = 3893 Ω, and capacitance C_0 = 200 pF per unity length were modified to the new values R_0 = 2280 Ω, and C_0 = 77 pF to obtain more suitable dimensions of the thick-film experimental samples. This modification only shifts the EFI impedance characteristic to 4.4-times higher frequencies without changing its shape. Generally, if the resistance R_0 and capacitance C_0 are changed to the new values $A{\cdot}R_0$ and $B{\cdot}C_0$, the impedance characteristic is shifted to $1/(A{\cdot}B)$-times higher frequencies without changing its shape.

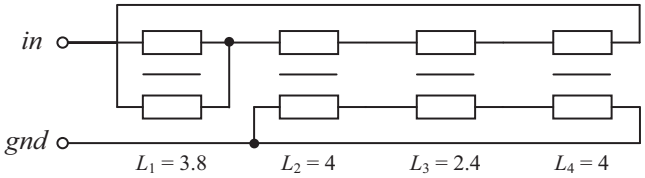

Fig. 9. Designed topology of EFI for verification.

The values R_0 and C_0 can be also used for rough estimate of impedance magnitude in the geometric center of the EFI frequency range (at frequency f_C) by the following formula:

$$|Z| \approx \sqrt{R_0^2 + \left(\frac{1}{2\pi f_C C_0}\right)^2}. \quad (20)$$

Setting a certain value of the impedance magnitude is possible after the synthesis by variation of the values R_0 and C_0. To obtain X-times higher impedance magnitude it is necessary to change R_0 to a new value $X{\cdot}R_0$ and C_0 to C_0/X. The phase impedance characteristic and the position of the characteristic on the frequency axis remain unchanged. In future work, it is planned to include in the synthesis the criterion of the impedance magnitude.

The theoretical EFI phase frequency characteristic displayed by the design program is shown in Fig. 10 in black line. To verify the correctness of the synthesis, the computer simulation of the impedance phase characteristics with R-C-NR structures modeled by lumped RC ladder circuits was performed. The results are also included in Fig. 10 in color lines whereas each line is obtained for different number of sections of the lumped RC structure. Apparently, these characteristics asymptotically converge to the synthesized phase response with the increasing number of RC sections. With an infinite number of RC sections, the frequency characteristics will be identical over a given frequency range, which proves the correctness of the R-C-NR EFI synthesis program.

Measurement of fabricated samples

Using the procedure described in [23], the synthesized EFI was fabricated in thick-film technology and its photograph is depicted in Fig. 11. More detailed information about the thick-film technology is beyond the scope of this paper. Those interested in the topic can refer, for example, to [29,30].

The measured phase characteristic is shown in Fig. 12 in red color, whereas the blue line shows the simulated phase with the layer resistances and capacitances really achieved in the produced samples. The difference of this simulated (blue) characteristic compared to the synthesized (black) one is caused particularly by the error in the resistance ratio N of the fabricated samples. The measured characteristic matches the simulated one at low frequencies, however the measured phase exhibits parasitic decrease at high frequencies. This phenomenon is primarily caused by parasitic

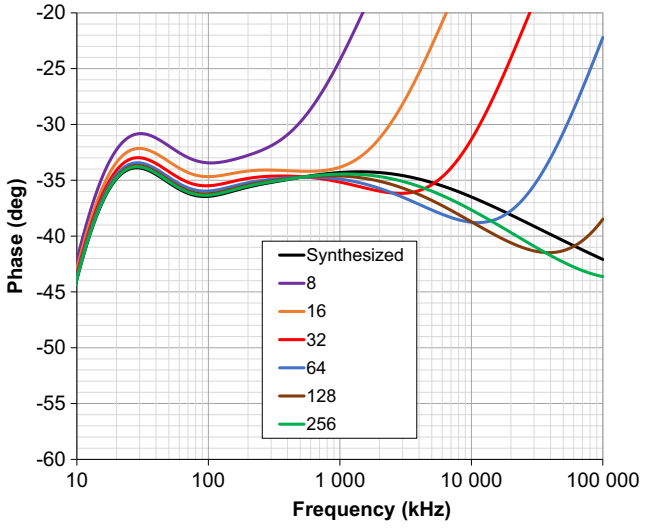

Fig. 10. Phase characteristics of the synthesized R-C-NR EFI (black) and of ladder RC structures with the stated number of sections (color).

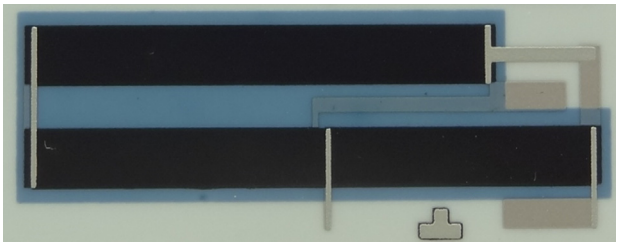

Fig. 11. Photograph of the fabricated thick-film EFI sample (dimensions approx. 43 × 16 mm).

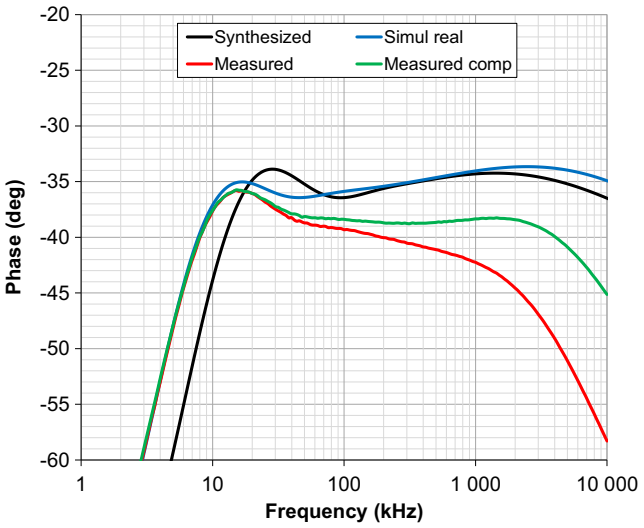

Fig. 12. Phase characteristics of the synthesized R-C-NR EFI (black), measured samples (red), simulated with the real properties of the manufactured materials (blue), and measured samples with compensation of contact parasitic capacitances (green).

capacitances of the resistive layer contacts which are above each other in the EFI prototype and do not have zero area. To compensate this parasitic effect the bottom resistive layer was extended by the contact width in order to move the bottom-layer contact and not let it overlap with the top-layer contact. The modification was practically verified on fabricated samples and resulted in improvement which is confirmed by the green characteristic in Fig. 12. The compensated samples show the impedance phase value between −36° to −39° in the frequency band from 8.7 kHz to 3 MHz which is 2.5 decades.

Although the verification of the synthesis procedure is presented by measurements of only one fabricated sample, the method presented in this paper has been verified also by our other designs; see [23,31].

Conclusions

The principle of EFI synthesis has been proposed, which consists in the use of interconnected segments of R-C-NR lines in a certain way. A description of the synthesis method has been given with a detailed explanation of the employed genetic algorithm. The synthesis method allows obtaining physically feasible designs with a range of fractional order alpha from approximately 0.06–0.94, i.e. the phase from 5° to 85° in the operating frequency range 3–3.5 decades. The example of EFI has been synthesized with impedance phase characteristics constant at 35°. The validity of the models employed in the synthesis program has been proven by the circuit simulation program and mainly by the experimentally fabricated

samples of EFIs using the thick-film technology. The measurements of the test samples show that impedance phase characteristics correspond with sufficient accuracy to the requirements specified during the synthesis and prove the functionality of the proposed design tool.

Compliance with Ethics Requirements

This article does not contain any studies with human or animal subjects.

Acknowledgements

The research was supported by the Czech Science Foundation project No. 19-24585S. This article is based upon work from COST Action CA15225. For the research, infrastructure of the SIX Center was used.

Declaration of Competing Interest

The authors declare that they have no known competing financial interests or personal relationships that could have appeared to influence the work reported in this paper.

References

[1] Shah ZM, Kathjoo MY, Khanday FA, Biswas K, Psychalinos C. A survey of single and multi-component Fractional-Order Elements (FOEs) and their applications. Microelectron J 2019;84:9–25. doi: https://doi.org/10.1016/j.mejo.2018.12.010.
[2] Adhikary A, Khanra M, Sen S, Biswas K. Realization of a carbon nanotube based electrochemical fractor; 2015. https://doi.org/978-1-4799-8391-9/15/$31.00.
[3] Elwakil A. Fractional-order circuits and systems: an emerging interdisciplinary research area. IEEE Circuits Syst Mag 2010;10(4):40–50.
[4] Tepljakov A. Fractional-order modeling and control of dynamic systems. Springer International Publishing. ISBN: 978-3-319-52949-3; 2017. https://doi.org/10.1007/978-3-319-52950-9.
[5] Tenreiro-Machado J, Lopes AM, Valério D, Galhano AM. Solved problems in dynamical systems and control. The IET; 2016.
[6] de Oliveira EC, Machado JAT. A review of definitions for fractional derivatives and integral. Math Probl Eng 2014;238459. doi: https://doi.org/10.1155/2014/238459.
[7] Biswas K, Sen S, Dutta PK. Realization of a constant phase element and its performance study in a differentiator circuit. IEEE Trans Circ Syst II 2006;53(9):802–6.
[8] Elshurafa M, Almadhoun N, Salama K, Alshareef H. Microscale electrostatic fractional-order capacitors using reduced graphene oxide percolated polymer composites. Appl Phys Lett 2013;102(23):232901–4.
[9] Buscarino A, Caponetto R, Di Pasquale G, Fortuna L, Graziani S, Pollicino A. Carbon Black based capacitive Fractional-order Element towards a new electronic device. AEU-Int J Electr Commun 2018;84:307–12.
[10] Caponetto R, Graziani S, Pappalardo FL, Sapuppo F. Experimental characterization of ionic polymer metal composite as a novel fractional-order element. Adv Math Phys 2013;2013:1–10.
[11] Agambayev A, Patole S, Bagci H, Salama KN. Tunable fractional-order capacitor using layered ferroelectric polymers. AIP Adv 2017;7:095202.
[12] Carlson GE, Halijak CA. Approximation of fractional-order capacitors $(1/s)^{1/n}$ by a regular Newton process. IEEE Trans Circ Theor 1964;11:210–3.
[13] Charef A, Sun HH, Tsao YY, Onaral B. Fractal system as represented by singularity function. IEEE Trans Automat Contr 1992;37(9):1465–70.
[14] Matsuda K, Fujii H. H∞ optimized wave-absorbing control: analytical and experimental results. J Guid Contr Dynam 1993;16(6):1146–53.
[15] Oustaloup A, Levron F, Mathieu B, Nanot FM. Frequency-band complex noninteger differenciator: characterization and synthesis. IEEE Trans Circ Syst I: Fundament Theor Appl 2000;47(1):25–39.
[16] El-Khazali R. On the biquadratic approximation of fractional-order Laplacian operators. Analog Integr Circ Signal Process 2015;82(3):503–17.
[17] Tsirimokou G. A systematic procedure for deriving RC networks of fractional-order elements emulators using MATLAB. AEU – Int J Electron Commun 2017;78:7–14. doi: https://doi.org/10.1016/j.aeue.2017.05.003.
[18] Kapoulea S. Design of fractional-order circuits with reduced spread of element values. Master thesis. RN: 1058034, 2018, available online: http://nemertes.lis.upatras.gr/jspui/bitstream/10889/11676/1/MScThesisKapoulea.pdf.
[19] Tsirimokou G, Psychalinos C, Elwakil AS. Emulation of a constant phase element using Operational Transconductance Amplifiers. Analog Integr Circ Sig Process 2015;85(3):413–23.
[20] Wyndrum RW Jr. The exact synthesis of distributed RC networks. Tech. Rept. 400-76. New York, N. Y.: Dept. of Elec. Engrg., New York University; May 1963.
[21] O'Shea R. Synthesis using distributed RC networks. IEEE Trans Circuit Theory 1965;12(4):546–54. doi: https://doi.org/10.1109/TCT.1965.1082508.
[22] Scanlan J, Rhodes J. Realizability and synthesis of a restricted class of distributed RC networks. IEEE Trans Circuit Theory 1965;12(4):577–85. doi: https://doi.org/10.1109/TCT.1965.1082511.
[23] Koton J, Kubanek D, Ushakov PA, Maksimov K. Synthesis of fractional-order elements using the RC-EDP approach. In: 2017 European conference on circuit theory and design (ECCTD), Catania, Italy; 2017. https://doi.org/10.1109/ecctd.2017.8093314.
[24] Gil'mutdinov A Kh, Ushakov PA. Physical implementation of elements with fractal impedance: state of the art and prospects. J Commun Technol Electron 2017;62(5):441–53. doi: https://doi.org/10.1134/S1064226917050060.
[25] Gilmutdinov AK, Ushakov PA, El-Khazali R. Fractal elements and their applications. Springer. ISBN: 978-3-319-45249-4; 2017. https://doi.org/10.1007/978-3-319-45249-4.
[26] Adhikary A, Choudhary S, Sen S. Optimal design for realizing a grounded fractional order inductor using GIC. IEEE Trans Circuits Syst I Regul Pap Aug. 2018;65(8):2411–21. doi: https://doi.org/10.1109/TCSI.2017.2787464.
[27] Handbook of Genetic Algorithms. Edited by Lawrence Davis. New York: Nostrand Reinhold; 1991. p. 385.
[28] Kaiser HR, Castro PS, Nichols AJ. Thin-film distributed parameter circuits. In: Space/aeronautics, R&D technical handbook. Vol. 38; 1962. p. E17–E23.
[29] Gilleo K. Polymer thick film: today's emerging technology for a clean environment tomorrow. USA: Van Nostrand Reinhold; 2016.
[30] White N. Thick films. In: Kasap S, Capper P, editors. Springer handbook of electronic and photonic materials. Springer; 2017.
[31] Ushakov P, Shadrin A, Kubanek D, Koton J. Passive fractional-order components based on resistive-capacitive circuits with distributed parameters. In: 2016 39th international conference on telecommunications and signal processing (TSP), Vienna; 2016. p. 638–42. https://doi.org/10.1109/TSP.2016.7760960.